

# On delay-partial-differential and delay-differential thermal models for variable pipe flow

Jens Wurm<sup>a</sup>, Simon Bachler<sup>a</sup>, Frank Woittennek<sup>a</sup>

<sup>a</sup>*Institute of Automation and Control Engineering,  
University for Health Sciences, Medical Informatics and Technology,  
Eduard Wallnöfer Zentrum 1, Hall in Tirol, Austria*

---

## Abstract

A new formulation of physical thermal models for variable plug flow through a pipe is proposed. The derived model is based on a commonly used one-dimensional distributed parameter model, which explicitly takes into account the heat capacity of the jacket of the pipe. The main result of the present contribution is the constitution of the equivalence of this model with a serial connection of a pure delay or transport system and another partial-differential equation (PDE), subsequently called delay-partial-differential equation (DPDE)-model. The means for obtaining the proposed model comprise operational calculus in the Laplace domain as well as classical theory of characteristics. The finite-dimensional approximation of the DPDE-model leads to a delay-differential equation (DDE)-system, which can be seen as a generalization of commonly used DDE-models consisting of a first-order low-pass filter subject to an input delay. The proposed model is compared to several alternative models in simulations and experimental studies.

*Keywords:* variable pipe flow, delay-differential equation, partial-differential equation, distributed parameter system, hyperbolic equation.

---

## 1. Introduction

Plug flow models are widely used in various applications to describe the thermal behavior of fluid flows through long pipes. Particular examples comprise solar desalination plants [1], district heating grids [2], the thermal behavior of catalysts [3, 4, 5], cooling loops of large gas engines [6], and solar thermal plants [7]. Commonly, one-dimensional partial-differential equations (PDEs) or delay-differential equations (DDEs) are used for these purposes. While the PDE-models are based directly on the mathematical description of the transport

---

*Email addresses:* [jens.wurm@umit.at](mailto:jens.wurm@umit.at) (Jens Wurm), [simon.bachler@umit.at](mailto:simon.bachler@umit.at) (Simon Bachler), [frank.woittennek@umit.at](mailto:frank.woittennek@umit.at) (Frank Woittennek)

Nomenclature				
$\Omega$	domain			
$r$	radial coordinate	[m]	<i>Time-dependent functions</i>	
$t$	time	[s]	$\dot{q}$	heat flux $\left[\frac{\text{W}}{\text{m}^2}\right]$
$z$	spatial coordinate	[m]	$\tau$	transport delay time [s]
<i>Constant parameters</i>			$T$	temperature $[\text{°C}]$
$\alpha$	heat transfer coefficient	$\left[\frac{\text{W}}{\text{m}^2 \text{K}}\right]$	$v$	velocity $\left[\frac{\text{m}}{\text{s}}\right]$
$\epsilon$	correction factor		<i>Indicies</i>	
$\lambda$	thermal conductivity	$\left[\frac{\text{W}}{\text{mK}}\right]$	$\infty$	ambient
$\mathbb{A}$	cross section surface	$[\text{m}^2]$	del	delayed
$\rho$	density	$\left[\frac{\text{kg}}{\text{m}^3}\right]$	in	input
$A$	surface area	$[\text{m}^2]$	m	medium
$c_p$	heat capacity	$\left[\frac{\text{J}}{\text{kgK}}\right]$	ma	medium-ambient
$l$	length of pipe	[m]	mw	medium-wall
$m$	mass	[kg]	out	output
$R$	radius	[m]	s	shell
$U$	perimeter	[m]	w	wall
			wa	wall-ambient

phenomena in combination with the heat exchange between fluid and wall, the DDE-models are obtained heuristically by augmenting simple physically motivated ordinary-differential equation (ODE)-models with additional delays in order to account for the transport phenomenon [8]. A physically based modeling approach for constant flow rate is presented in [4, 5] describing the thermal behavior of an oxidation catalyst. Moreover, an approximation of the PDE-model by an corresponding diffusion equation is discussed in [9]. In contrast a data driven model is introduced by [10]. To the best knowledge of the authors no consistently physically based DDE-modeling approach has been published yet for the variable flow case. However, thanks to their simple structure DDE-models have been proven to be well suited in control applications [11, 12, 13].

These observations motivate the derivation of generalized DDE-models, which constitute one of the main results of the present work. The second contribution consists in an alternative PDE-model, which separates the transport process from the filtering dynamics of the pipe.

Starting from a detailed one-dimensional PDE-model for the fluid inside the pipe and a two-dimensional PDE-model for the wall an one-dimensional PDE-model is derived. The latter approximates both the transport process of the fluid and the dynamics of the heat exchange between wall and fluid. It constitutes the

basis of all models developed in the present contribution. Originating from this model the well known ODE-model is derived, which can be intuitively adapted to the common used standard DDE-approach. The new pipe model proposed in the present contribution is also based on the one-dimensional PDE-model. It combines a PDE- and DDE-model and is named delay-partial-differential equation (DPDE)-model due to its particular structure and is suitable for both constant and variable flow rate. An approximation of the new DPDE-model reveals the new generalized DDE-models with a similar structure as the common used one. Finally, the different models are compared against each other and validated by measurements.

The contribution is structured as follows: The standard pipe models are introduced in Section 2. The new pipe model is presented and linked to the standard approaches in Section 3. In Section 4 the general DDE-approaches are derived, analyzed and optimized. All models are compared by simulation studies and validated by measurements in Section 5.

## 2. Pipe Models

Two models of different type describing the thermal behavior of a plug flow in a pipe are presented within this section. Figure 1 shows the considered pipe of length  $l$  with inner and outer radii  $R_m$  and  $R_w$ . The medium temperature is denoted by  $T_m$ ,  $T_w$  is the wall temperature, and  $T_\infty$  describes the ambient temperature. The input temperature profile is  $T_{m,in}$ , the velocity of the medium is  $v_m$ , and  $\dot{q}$  stands for the heat flux between medium, wall, and ambient. For the modeling an (i) incompressible medium with (ii) a radially constant temperature and velocity profile due to turbulent flow is assumed. Furthermore, thanks to a sufficiently large medium velocity (iii) the thermal conduction in flow direction is neglected for both the wall and the medium, and (iv) all material parameter are assumed to be spatially and temporally constant.

### 2.1. Partial-differential equation-approach

For the sake of simplicity<sup>1</sup> the pipe is assumed cylindrical with cross section  $\mathbb{A}_p \subset \mathbb{R}^2$ . In the following the equations are written in cylindrical coordinates with  $r$  the radial coordinate,  $z$  the axial coordinate. The angular coordinate is dropped due to a symmetry assumption. The pipe shown in Figure 1 can be separated into a medium and a wall part, which can be treated separately.

#### 2.1.1. Medium

Taking into account Assumption (ii), a constant temperature profile over the cross section  $\mathbb{A}_m$  of the medium can be assumed. Moreover, considering

---

<sup>1</sup>Note that the further findings and calculations are not restricted to the cylindrical geometry but can be adapted to arbitrary cross-sections. However, the generalization would require some notational and computational effort.

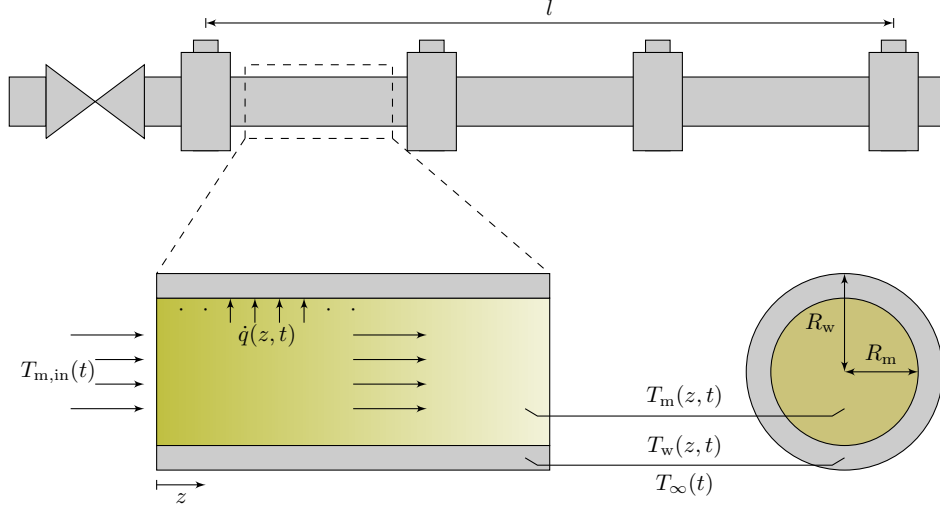


Figure 1: Sketch of pipe test rig and used variables.

Assumption (iii) leads to the well known one-dimensional transport-equation describing the fluid flow in  $z$ -direction (see, e.g., [14]):

$$A_m c_{p,m} \rho_m (\partial_t T_m(z, t) + v_m(t) \partial_z T_m(z, t)) = -2\pi R_m \dot{q}(R_m, z, t), \quad (1)$$

with the specific heat capacity  $c_{p,m}$  and the density  $\rho_m$  of the medium. The heat flux  $\dot{q}(R_m, z, t)$  from the medium into the wall is detailed below in (3b). Moreover, the corresponding inflow boundary condition and the initial condition are given by

$$T_m(0, t) = T_{m,\text{in}}(t), \quad T_m(z, 0) = T_{m,0}(z),$$

respectively, with the input temperature  $T_{m,\text{in}}$  and the initial temperature profile  $z \mapsto T_{m,0}(z)$ .

### 2.1.2. Wall

The evolution of the temperature distribution within the wall is described by the heat equation [15, p. 87], which reads in cylindrical coordinates:

$$\rho_w c_{p,w} \partial_t T_w(r, z, t) = -\frac{1}{r} \partial_r (r \dot{q}(r, z, t)), \quad \dot{q}(r, z, t) = -\lambda_w \partial_r T_w(r, z, t). \quad (2)$$

Here  $\lambda_w$  denotes the thermal conductivity of the wall and  $\dot{q}$  is the radial component of the heat flux within the wall. Above, the possible dependency of the wall temperature on an angular coordinate has been dropped for symmetry reasons. Moreover, the heat flux in axial direction has been neglected in view of Assumption (iii).

The boundary conditions for the shell surface are given by Fourier's Law

$$-\dot{q}(R_w, z, t) = \lambda_w \partial_r T_w(R_w, z, t) = -\alpha_{wa}(T_w(R_w, z, t) - T_\infty(t)), \quad (3a)$$

$$-\dot{q}(R_m, z, t) = \lambda_w \partial_r T_w(R_m, z, t) = \alpha_{mw}(T_w(R_m, z, t) - T_m(z, t)). \quad (3b)$$

In the above equations linear heat transfer between the wall and the medium respectively the medium and the ambient is assumed. The respective heat transfer coefficients are denoted by  $\alpha_{mw}$  and  $\alpha_{wa}$ . Finally, the initial conditions read

$$T_w(r, z, 0) = T_{w,0}(r, z).$$

### 2.1.3. Overall one-dimensional model

The complete one-dimensional model is derived by combining the models for the medium and the wall. To this end, the wall temperature model is reduced to a one-dimensional model by averaging the wall temperature over the area  $A_w = (R_w^2 - R_m^2)\pi$  of the cross sectional surface  $\mathbb{A}_w$ :

$$\bar{T}_w(z, t) = \frac{2\pi}{A_w} \int_{R_m}^{R_w} T_w(r, z, t) r dr. \quad (4)$$

Similarly, integrating the PDE-model of the wall temperature (2) over  $\mathbb{A}_w$  yields

$$\begin{aligned} A_w \rho_w c_{p,w} \partial_t \bar{T}_w(z, t) &= 2\pi \lambda_w \left[ r \partial_r T_w(r, z, t) \right]_{R_m}^{R_w} \\ &= 2\pi \lambda_w \left[ R_w \partial_r T_w(R_w, z, t) - R_m \partial_r T_w(R_m, z, t) \right] \end{aligned}$$

with the averaged wall temperature given by (4). Substituting the boundary derivatives on the right hand side by the boundary conditions (3) reveals

$$\begin{aligned} A_w \rho_w c_{p,w} \partial_t \bar{T}_w(z, t) &= 2\pi \left[ R_w \alpha_{wa} (T_\infty(t) - T_w(R_w, z, t)) \right. \\ &\quad \left. + R_m \alpha_{mw} (T_m(z, t) - T_w(R_m, z, t)) \right]. \end{aligned}$$

Finally, the boundary wall temperature is approximated by the average temperature (4). This leads to the one-dimensional model

$$\begin{aligned} A_w \rho_w c_{p,w} \partial_t \bar{T}_w(z, t) &= U_w \bar{\alpha}_{wa} (T_\infty(t) - \bar{T}_w(z, t)) + U_m \bar{\alpha}_{mw} (T_m(z, t) - \bar{T}_w(z, t)) \end{aligned}$$

for the pipe jacket, where the new overall heat transfer coefficients  $\bar{\alpha}_{mw}$  and  $\bar{\alpha}_{wa}$  are defined by

$$\begin{aligned} \frac{1}{\bar{\alpha}_{mw}} &= \frac{1}{\alpha_{mw}} + \frac{\bar{R}_m}{\lambda_w}, \\ \frac{1}{\bar{\alpha}_{wa}} &= \frac{1}{\alpha_{wa}} + \frac{\bar{R}_w}{\lambda_w}, \end{aligned}$$

with

$$\begin{aligned}\bar{R}_m &= R_m \left( \frac{R_w^2}{R_w^2 - R_m^2} \ln \left( \frac{R_w}{R_m} \right) - \frac{1}{2} \right), \\ \bar{R}_w &= R_m \left( -\frac{R_m^2}{R_w^2 - R_m^2} \ln \left( \frac{R_w}{R_m} \right) + \frac{1}{2} \right)\end{aligned}$$

for a cylindrical pipe profile. They are chosen in such a way, that the substitution is exact in the stationary regime (cf. Appendix A). Moreover, the perimeters  $U_m = 2\pi R_m$  and  $U_w = 2\pi R_w$  are introduced for ease of notation. The same approximation is applied to the heat flux (3b) appearing on the right hand side of the one-dimensional PDE-model (1) for the medium temperature. Thus, (1) can be rewritten as

$$c_{p,m} \rho_m (\partial_t T_m(z, t) + v_m(t) \partial_z T_m(z, t)) = \frac{U_m}{A_m} \bar{\alpha}_{mw} (\bar{T}_w(z, t) - T_m(z, t)).$$

Finally, the thermal behavior of a plug flow through a pipe can be described by the one-dimensional PDE-system

$$v_m(t) \partial_z T_m(z, t) + \partial_t T_m(z, t) = h_1 (T_w(z, t) - T_m(z, t)) \quad (5a)$$

$$\begin{aligned}\partial_t T_w(z, t) &= h_2 (T_m(z, t) - T_w(z, t)) \\ &\quad - h_3 (T_w(z, t) - T_\infty(t))\end{aligned} \quad (5b)$$

with boundary condition

$$T_m(0, t) = T_{m,\text{in}}(t) \quad (5c)$$

and the initial conditions

$$T_m(z, 0) = T_{m,0}(z), \quad T_w(z, 0) = T_{w,0}(z). \quad (5d)$$

The physical parameters are collected in

$$h_1 = \frac{U_m}{A_m} \frac{\bar{\alpha}_{mw}}{\rho_m c_{p,m}}, \quad h_2 = \frac{U_m}{A_w} \frac{\bar{\alpha}_{mw}}{\rho_w c_{p,w}}, \quad h_3 = \frac{U_w}{A_w} \frac{\bar{\alpha}_{wa}}{\rho_w c_{p,w}}.$$

Therein and below the averaged wall temperature  $\bar{T}_w$  is denoted by  $T_w$  for notational simplicity.

**Remark.** Since the convection boundary layer between the medium and the wall varies at different velocities the heat transfer coefficients may dependent on velocity [15]. Hence, the PDE-model (5) can be extended to

$$\begin{aligned}v_m(t) \partial_z T_m(z, t) + \partial_t T_m(z, t) &= h_1 (v_m(t)) (T_w(z, t) - T_m(z, t)) \\ \partial_t T_w(z, t) &= h_2 (v_m(t)) (T_m(z, t) - T_w(z, t)) \\ &\quad - h_3 (T_w(z, t) - T_\infty(t)).\end{aligned}$$

Assuming an affine velocity dependence of  $\bar{\alpha}_{mw}$  with the slope  $\alpha_{mw,1}$  (unit  $W s/(m^3 K)$ ) and the intercept  $\alpha_{mw,0}$  (unit  $W/(m^2 K)$ ) the heat transfer coefficients are given by:

$$h_1(v_m(t)) = \frac{U_m}{A_m} \frac{\alpha_{mw,0} + \alpha_{mw,1}v_m(t)}{\rho_m c_{p,m}},$$

$$h_2(v_m(t)) = \frac{U_m}{A_w} \frac{\alpha_{mw,0} + \alpha_{mw,1}v_m(t)}{\rho_w c_{p,w}}.$$

## 2.2. Ordinary-differential equation-approach

If the output temperature of the pipe is of particular interest and transport delays do not play a significant role simple ODE-models can be employed instead of the above derived PDE. Such models are preferred for example for automotive cooling loops (cf. [16]). The derivation of the model equations starting from (1) is sketched below.

In contrast to the presented PDE-models, the dynamics of the wall temperature is not explicitly taken into account. Hence, a heat flux

$$\dot{q}(z, t) = -\alpha_{ma}(T_m(z, t) - T_\infty(t)) \quad (6)$$

is observed between medium and ambient instead of (3), with an overall heat transfer coefficient (cf. [17, p. 31 ff.] )

$$\frac{1}{\alpha_{ma}} = \frac{1}{\alpha_{mw}} + \frac{1}{\alpha_{wa}} + \frac{R_m}{\lambda_w} \ln\left(\frac{R_w}{R_m}\right). \quad (7)$$

Thus, the simplified one-dimensional PDE-model gets<sup>2</sup>

$$c_{p,m}\rho_m [v_m(t)\partial_z T_m(z, t) + \partial_t T_m(z, t)] = \frac{U_w}{A_m} \alpha_{ma}(T_\infty(t) - T_m(z, t)), \quad (8)$$

with the boundary condition

$$T_m(0, t) = T_{m,in}(t)$$

and the initial condition

$$T_m(z, 0) = T_{m,0}(z).$$

The simplified PDE-model (8) can be interpreted as a further approximation of the PDE-model (5), where the dynamics of the wall temperature are neglected and the new overall heat transfer coefficient (7) is derived based on the stationary wall temperature profile.

---

<sup>2</sup>Note that the heat capacity of the wall can be accounted for by an additional coefficient in front of  $\partial_t T_m(z, t)$  (see (11))

In a further approximation step a spatial discretization of (8) with the simple difference quotient

$$(\partial_z T_m)(l, t) \approx \frac{1}{l} (T_m(l, t) - T_{m,\text{in}}(t))$$

leads to the ODE (with  $T_m(t) := T_m(l, t)$ )

$$d_t T_m(t) = \frac{v_m(t)}{l} (T_{m,\text{in}}(t) - T_m(t)) + h_4 (T_\infty(t) - T_m(t)) \quad (9)$$

describing the average medium temperature of the pipe. Therein

$$h_4 = \frac{U_w}{A_m} \frac{\alpha_{\text{ma}}}{c_{p,m} \rho_m}.$$

Due to constant material parameters (cf. Assumption (iv)) (9) can easily be generalized to

$$d_t T_m(t) = \frac{v_m(t)}{l} (T_{m,\text{in}}(t) - T_m(t)) + \frac{\alpha_{\text{ma}} A_s}{c_{p,m} m_m} (T_\infty(t) - T_m(t)),$$

where  $m_m$  describes the mass of the medium inside the pipe and  $A_s$  the shell surface area.<sup>3</sup> The latter model is used for configurations allowing for the neglect of the transport phenomenon, e.g. in automotive cooling loops, where the pipes are rather short [16].

### 2.3. Delay-differential equation-approach

If the transport delays within the medium cannot be neglected, as in solar field applications [7, 1] or systems with long pipes [11, 6], the simple ODE-approach (9) is intuitively complemented by the variable transport delay  $\tau$ , implicitly defined by:

$$\int_{t-\tau(t)}^t v_m(\zeta) d\zeta = l.$$

This way, one obtains the DDE-model

$$\partial_t T_m(t) = \frac{v_m(t)}{l} (T_{m,\text{in}}(t - \tau(t)) - T_m(t)) + h_4 (T_\infty(t) - T_m(t)) \quad (10)$$

as discussed in [8].

Though such models have been proven to be useful in applications within their derivation the transport phenomenon is considered twice: After approximating the transport equation by means of a first-order ODE and abandon the

---

<sup>3</sup>Note, that in a system theoretical sense the ODE representation of the pipe equals a filtering of the input and ambient temperature with a first-order low-pass filter.



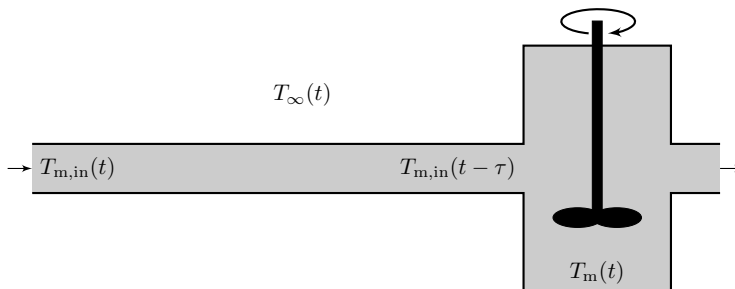


Figure 2: Physical interpretation of the classical DDE-pipe model.

transport delay, the latter will be introduced again in a consecutive modeling step. A physical interpretation of the obtained DDE-model for a constant velocity is depicted in Figure 2. It shows an ideal pipe (pure convection) connected to an ideally stirred tank, which models the heat dissipation as well as the heat capacity of the wall. However, at first glance the separation of the transport process and the dynamics does not seem reasonable. In [18] it is shown that a PDE-approach, which does not explicitly consider the heat capacity of the wall does not reveal a pipe model like (10). Nevertheless, the heat capacity of the wall can be considered heuristically by extending the DDE-model (10) with an additional correction factor  $\epsilon$  to

$$\epsilon \partial_t T_m(t) = \frac{v_m(t)}{l} (T_{m,\text{in}}(t - \tau(t)) - T_m(t)) + \frac{\alpha_{\text{ma}} A_s}{c_{p,m} m_m} (T_{\infty}(t) - T_m(t)), \quad (11)$$

as proposed in [18]. However, when explicitly taking into account the heat capacity of the wall similar results may be obtained by a first order approximation of the transfer function in the frequency domain for constant flow rates [4, 5].

### 3. Delay-Partial-Differential-Equation Model

The new modeling approach described below is based on the one-dimensional PDE (5) for plug flow through a pipe with additional heat storage within the wall and heat transfer between medium and wall respectively wall and ambient. Due to its particular structure separating the transport phenomena within the medium from the wall dynamics the new model is named DPDE-model in the following. In a first step the basic ideas are sketched under the simplifying assumptions of a constant flow rate and a perfectly isolated pipe in the Laplace domain. Therefore, the transfer function of the one-dimensional pipe model (5) is analyzed. This part basically restates the results already presented in [4, 5]. Based on that findings the new DPDE-model is introduced in form of a second order PDE with delayed boundary condition. Afterwards, this formulation is generalized by taking into account the heat loss to the ambient and time dependent flow velocities.

### 3.1. Constant flow rate and perfect isolation

Assuming a constant flow rate  $v_m$  of the fluid, perfect isolation ( $h_3 = 0$ ), and homogeneous initial conditions<sup>4</sup>,  $T_m(z, 0) = T_w(z, 0) = 0$ , the boundary value problem (BVP) (5) can be transformed into the Laplace domain

$$v_m \partial_z \widehat{T}_m(z, s) + s \widehat{T}_m(z, s) = h_1 \left( \widehat{T}_w(z, s) - \widehat{T}_m(z, s) \right) \quad (12a)$$

$$s \widehat{T}_w(z, s) = h_2 \left( \widehat{T}_m(z, s) - \widehat{T}_w(z, s) \right) \quad (12b)$$

with the Laplace transforms  $\widehat{T}_m$  and  $\widehat{T}_w$  of the corresponding temperatures [4, 5]. Eliminating the wall temperature from (12) one obtains

$$v_m \partial_z \widehat{T}_m(z, s) = \zeta(s) \widehat{T}_m(z, s), \quad \zeta(s) = \frac{h_1 h_2}{s + h_2} - h_1 - s. \quad (13)$$

The solution of (13) is given by

$$\widehat{T}_m(z, s) = G_{T_m}(z, s) \widehat{T}_m(0, s), \quad G_{T_m}(z, s) = \exp\left(\frac{z}{v_m} \zeta(s)\right).$$

The transfer function  $G_{T_m}(z, s)$  can be easily split up into three multiplicative parts given by

$$G_1(z, s) = \exp\left(-s \frac{z}{v_m}\right), \quad G_2(z) = \exp\left(-h_1 \frac{z}{v_m}\right), \quad G_3(z, s) = \exp\left(\frac{z}{v_m} \frac{h_1 h_2}{s + h_2}\right).$$

Therein,  $G_1(s)$  corresponds to a pure spatially dependent time delay and  $G_2(s)$  is a spatially dependent scaling factor. Moreover, as explained below,  $G_3(z, s)$  can be interpreted as an infinite-dimensional filter without any time delay. As a consequence, the overall structure of the transfer function is similar to the structure of the DDE-model (10) discussed in Section 2.3. The main difference is constituted by the filter part  $G_3(z, s)$  replacing the simple first-order low-pass filter in the DDE-model (10). In order to compute the impulse response of this filter, i.e., transforming the input-output relation associated with  $G_3(z, s)$  into the time domain, the transfer function is expanded into a power series:

$$G_3(z, s) = 1 + \sum_{n=1}^{\infty} \frac{1}{n!} \left( \frac{z}{v_m} \frac{h_1 h_2}{s + h_2} \right)^n. \quad (14)$$

---

<sup>4</sup>At this point we are primarily interested in the input-output behaviour, i.e., in computing the transfer function. Consequently inhomogeneous initial conditions can be assumed without loss of generality. In contrast the DPDE-model computed at the end of the subsection constitutes a particular realization of this transfer function only. However, the time domain computations in Section 3.2 show that this DPDE-model is indeed equivalent to the original PDE description.

The sum within the latter expression can be interpreted as a parallel connection of an infinite number of low-pass filters of increasing order. Element-wise computation of the inverse Laplace transform of (14) yields the desired, spatially dependent impulse response:

$$\begin{aligned} g_3(z, t) &= \delta(t) + \exp(-h_2 t) \sum_{n=0}^{\infty} \frac{(Kz)^{n+1} t^n}{(n+1)!n!} \\ &= \delta(t) + \exp(-h_2 t) \sqrt{Kz} \sum_{n=0}^{\infty} \frac{1}{(n+1)!n!} \sqrt{Kz}^{2n+1}, \end{aligned} \quad (15)$$

with  $K = \frac{h_1 h_2}{v_m}$  and the Dirac delta distribution  $\delta$ . With the substitution  $x = 2\sqrt{Kz}t$  the infinite sum within the above expression corresponds to the well known series expansion of the modified Bessel function of first order:

$$x \mapsto \mathbf{I}_1(x) = \sum_{n=0}^{\infty} \frac{1}{(n+1)!n!} \left(\frac{x}{2}\right)^{2n+1}.$$

As a result the impulse response (15) can be rewritten as (cf. [5])

$$g_3(z, t) = \delta(t) + \exp(-h_2 t) \sqrt{\frac{z}{v_m} \frac{h_1 h_2}{t}} \mathbf{I}_1 \left( 2\sqrt{\frac{h_1 h_2 z t}{v_m}} \right). \quad (16)$$

With the above computed impulse response (16) in the time domain the input-output relation corresponding to  $G_F(z, s) = G_2(z)G_3(z, s)$  is given by the convolution ( $\star$ ) of  $g_F(z, t) = G_2(z)g_3(z, t)$  and the delayed input  $T_{m,\text{in}}^{\text{del}}(\bullet)$  by:

$$T_m^{\text{del}}(z, \bullet) = g_F(z, \bullet) \star T_{m,\text{in}}^{\text{del}}(\bullet) \quad (17)$$

at a specific time  $\bullet$ . Therein,  $(z, t) \mapsto T_m^{\text{del}}(z, t)$  and  $t \mapsto T_{m,\text{in}}^{\text{del}}(t)$  can be seen as delayed temperature profiles, which coincide with  $T_m$

$$T_m^{\text{del}}(z, t) = T_m(z, t - \tau(l - z)), \quad (18)$$

respectively  $T_{m,\text{in}}$

$$T_{m,\text{in}}^{\text{del}}(t) = T_m^{\text{del}}(0, t) = T_{m,\text{in}}(t - \tau(l)) \quad (19)$$

up to the spatially dependent transport delay imposed by  $G_1(z, s)$ , i.e.,

$$\tau(z) = \frac{z}{v_m}. \quad (20)$$

Observe that at the outflow boundary  $z = l$  the delayed temperature corresponds to the actual temperature:

$$T_m(l, t) = T_m^{\text{del}}(l, t). \quad (21)$$

In view of a intended numerical implementation of the DPDE-model a realization of the transfer function (17) as a BVP has to be derived. This can be either achieved by means of the substitution

$$\widehat{T}_m(z, s) = \exp(s\tau(l-z))\widehat{T}_m^{\text{del}}(z, s), \quad \widehat{T}_{m,\text{in}}(s) = \exp(s\tau(l))\widehat{T}_{m,\text{in}}^{\text{del}}(s)$$

in (13) or, equivalently, by differentiating the relation

$$\widehat{T}_m^{\text{del}}(z, s) = G_F(z, s)\widehat{T}_{m,\text{in}}^{\text{del}}(s), \quad G_F(z, s) = G_2(z)G_3(z, s)$$

in the Laplace domain. Both approaches yield the ordinary BVP

$$v_m(s + h_2)\partial_z\widehat{T}_m^{\text{del}}(z, s) + h_1s\widehat{T}_m^{\text{del}}(z, s) = 0, \quad \widehat{T}_m^{\text{del}}(0, s) = \widehat{T}_{m,\text{in}}^{\text{del}}(s). \quad (22)$$

Translating this relation into the time domain leads to the desired PDE

$$v_m(\partial_t + h_2)\partial_z T_m^{\text{del}}(z, t) + h_1\partial_t T_m^{\text{del}}(z, t) = 0, \quad (23)$$

which, together with the delayed inflow boundary condition (19) and the output equation (21) constitutes the complete new DPDE-model under the given simplifying assumptions. Note that, the presented ideas immediately generalize to the non isolated case.

### 3.2. Variable flow rate

In case of variable flow rates the formal computations in the Laplace domain are not applicable due to the time variance of the system considered. Nevertheless, as shown below the ideas generalize even to a time varying setting in a similar way. To this end the spatial dependence delay introduced within the previous section is replaced by time and spatial depending transport delay, which can be described by the integral equation (similar definition for pure transport processes can be found e.g. in [8, 19]):

$$\int_{t-\tau(l-z,t)}^t v_m(\zeta) d\zeta = \int_z^l d\nu = l - z. \quad (24)$$

Therein,  $\tau(l-z, t)$  denotes the time which a portion of fluid arriving at a certain time  $t$  at the outflow  $z = l$  has traveled from the point  $l - z$ . Similarly as in (18) the delayed temperature

$$T_*^{\text{del}}(z, t) = T_*(z, t - \tau(l-z, t)) = T_*(z, \varphi(z, t))$$

is introduced, where the abbreviation  $\varphi(z, t) = t - \tau(l-z, t)$  has been used for convenience and  $*$  may be replaced by  $m$ ,  $w$  or  $\infty$ . The temporal and spatial derivatives of these delayed quantities are given by

$$\partial_t T_*^{\text{del}}(z, t) = \partial_t \varphi(z, t) \partial_\varphi T_*(z, \varphi(z, t)), \quad (25a)$$

$$\partial_z T_*^{\text{del}}(z, t) = \partial_z T_*(z, \varphi(z, t)) + \partial_z \varphi(z, t) \partial_\varphi T_*(z, \varphi(z, t)). \quad (25b)$$

Therein, the derivatives of  $\varphi$  w.r.t.  $z$  and  $t$  follow by differentiating (24) and the usage of the Leibniz integral rule, i.e., from

$$\partial_z \int_{\varphi(z,t)}^t v_m(\zeta) d\zeta = -\partial_z \varphi(z,t) v_m^{\text{del}}(z,t) = -1, \quad (26a)$$

$$\partial_t \int_{\varphi(z,t)}^t v_m(\zeta) d\zeta = v_m(t) - \partial_t \varphi(z,t) v_m^{\text{del}}(z,t) = 0 \quad (26b)$$

with the delayed velocity

$$v_m^{\text{del}}(z,t) = v_m(\varphi(z,t)).$$

Taking into account (26), (25) can be simplified to

$$\begin{aligned} \partial_t T_*^{\text{del}}(z,t) &= \frac{v_m(t)}{v_m^{\text{del}}(z,t)} \partial_\varphi T_*(z, \varphi(z,t)), \\ \partial_z T_*^{\text{del}}(z,t) &= \partial_z T_*(z, \varphi(z,t)) + \frac{1}{v_m^{\text{del}}(z,t)} \partial_\varphi T_*(z, \varphi(z,t)). \end{aligned}$$

Substitution of (25) into the delayed version of (5) yields

$$v_m^{\text{del}}(z,t) \partial_z T_m^{\text{del}}(z,t) = h_1 (T_w^{\text{del}}(z,t) - T_m^{\text{del}}(z,t)) \quad (27a)$$

$$\begin{aligned} \partial_t T_w^{\text{del}}(z,t) &= \frac{v_m(t)}{v_m^{\text{del}}(z,t)} \left( h_2 (T_m^{\text{del}}(z,t) - T_w^{\text{del}}(z,t)) \right. \\ &\quad \left. + h_3 (T_\infty^{\text{del}}(z,t) - T_m^{\text{del}}(z,t)) \right). \end{aligned} \quad (27b)$$

Solving (27a) for  $T_w^{\text{del}}$

$$T_w^{\text{del}}(z,t) = \frac{v_m^{\text{del}}(z,t)}{h_1} \partial_z T_m^{\text{del}}(z,t) + T_m^{\text{del}}(z,t) \quad (28)$$

and substituting the resulting expression into (27b) finally yields the desired DPDE (cf. (30a))

$$\begin{aligned} &v_m^{\text{del}}(z,t) \partial_{tz} T_m^{\text{del}}(z,t) + h_1 \partial_t T_m^{\text{del}}(z,t) + \partial_t v_m^{\text{del}}(z,t) \partial_z T_m^{\text{del}}(z,t) \\ &\quad + (h_2 + h_3) v_m(t) \partial_z T_m^{\text{del}}(z,t) + h_1 h_3 \frac{v_m(t)}{v_m^{\text{del}}(z,t)} T_m^{\text{del}}(z,t) \\ &= h_1 h_3 \frac{v_m(t)}{v_m^{\text{del}}(z,t)} T_\infty^{\text{del}}(z,t) \end{aligned} \quad (29a)$$

with the boundary condition

$$T_m^{\text{del}}(0,t) = T_{m,\text{in}}^{\text{del}}(t) = T_{m,\text{in}}(t - \tau(l,t)). \quad (29b)$$

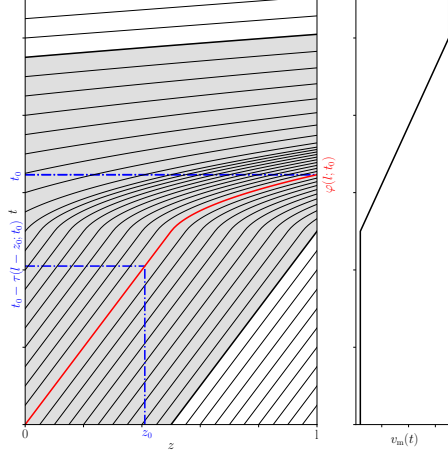


Figure 3: Characteristics for a time variant flow regime.

For constant flow the DPDE model (29) simplifies to

$$\begin{aligned} \partial_{tz} T_m^{\text{del}}(z, t) + (h_2 + h_3) \partial_z T_m^{\text{del}}(z, t) \\ = \frac{h_1}{v_m} (h_3 (T_\infty^{\text{del}}(z, t) - T_m^{\text{del}}(z, t)) - \partial_t T_m^{\text{del}}(z, t)), \end{aligned} \quad (30a)$$

with

$$T_m^{\text{del}}(0, t) = T_{m, \text{in}}(t - \tau(l)), \quad T_m(l, t) = T_m^{\text{del}}(l, t). \quad (30b)$$

Moreover, in the particular case  $h_3 = 0$ , i.e., for the perfectly isolated pipe, (29) reduces to

$$\begin{aligned} v_m^{\text{del}}(z, t) \partial_{tz} T_m^{\text{del}}(z, t) + h_1 \partial_t T_m^{\text{del}}(z, t) + \partial_t v_m^{\text{del}}(z, t) \partial_z T_m^{\text{del}}(z, t) \\ + h_2 v_m(t) \partial_z T_m^{\text{del}}(z, t) = 0. \end{aligned}$$

Remark, that the above performed computations correspond to the evaluation of the system (5) on the characteristic projections of (5a) (cf. [20, 21]). In this context, each of the functions

$$[0, l] \ni z \mapsto \varphi(z, t) \in \mathbb{R}, \quad t \in \mathbb{R}$$

simply corresponds to the particular characteristic projection  $z \mapsto (z, \varphi(z, t))$  in the  $(z, t)$ -plane containing the point  $(l, t)$ . Figure 3 depicts the characteristic projections for a variable flow rate. In the following section the approximation of the DPDE-model to a first order DDE is shown.

#### 4. Approximation as Delay-Differential Equation

Within this section approximation schemes for the derived models are introduced. These approximations form the basis for the subsequent numerical

studies in Section 5. Moreover, the advantages and disadvantages of the proposed models are discussed.

All PDE-models are semi-discretized w.r.t. the spatial variable only. This is achieved by means of the finite difference method (FDM), i.e., by approximating the spatial derivatives by backward differences:

$$(\partial_z T_*) (z_i, t) \approx \frac{T_{*,i}(t) - T_{*,i-1}(t)}{z_i - z_{i-1}}, \quad i \in [1, n].$$

Therein,  $n$  specifies the number of  $n + 1$  sampling points  $z_0, \dots, z_n$ . As a consequence the PDE-models are approximated by a system consisting of  $n$  ODEs respectively DDEs. For the sake of simplicity, these computations are discussed for constant flow rates only, i.e., for (30).

The simplest approximation of the DPDE-model (30) with  $n = 1$  provides the link to the DDE-model (10). It corresponds to a discretization of the spatial derivative by the difference

$$(\partial_z T_m^{\text{del}}) (l, t) \approx \frac{1}{l} (T_m^{\text{del}}(l, t) - T_m^{\text{del}}(0, t)) = \frac{1}{l} (T_m(t) - T_{m,\text{in}}(t - \tau(l))).$$

Taking the input boundary condition into account, (30) leads to

$$\begin{aligned} \partial_t T_m(t) &= k_1 (T_{m,\text{in}}(t - \tau(l)) - T_m(t)) + k_2 (T_\infty(t) - T_m(t)) \\ &\quad + k_3 \partial_t T_{m,\text{in}}(t - \tau(l)), \end{aligned} \quad (31)$$

with the constants

$$k_1 = \frac{(h_2 + h_3)v_m}{v_m + h_1 l}, \quad k_2 = \frac{h_1 h_3 l}{v_m + h_1 l}, \quad k_3 = \frac{v_m}{v_m + h_1 l}.$$

Eqn. (31) reveals a similar structure as the heuristic DDE-model (10).<sup>5</sup> Apart from the different constants  $k_i$  there is an additional term involving input temporal derivative, which is induced by a feedthrough of the input temperature in the physical based approach. However, if the length of the pipe is sufficiently large compared to the velocity of the medium or a sufficiently high heat exchange between medium and wall is present, this term can be neglected. In this case (31) reduces to the DDE-model (10). Otherwise, the remaining term can be treated as described below for higher approximation orders.

Approximating the DPDE-model (30) by the backward difference leads to

$$\begin{aligned} d_t (T_{m,i}^{\text{del}}(t) - k_3 T_{m,i-1}^{\text{del}}(t)) &= k_1 (T_{m,i-1}^{\text{del}}(t) - T_{m,i}^{\text{del}}(t)) \\ &\quad + k_2 (T_{\infty,i}^{\text{del}}(t) - T_{m,i}^{\text{del}}(t)), \end{aligned} \quad (32)$$

---

<sup>5</sup>Note that for the time variant case one reveals the time depending coefficients

$$k_1(t) = \frac{\partial_t v_m(t) + (h_2 + h_3)v_m(t)}{v_m(t) + h_1 l}, \quad k_2(t) = \frac{h_1 h_3 l}{v_m(t) + h_1 l}, \quad k_3(t) = \frac{v_m(t)}{v_m(t) + h_1 l},$$

and the time variant delay  $\tau(l, t)$ .

with the constants

$$k_1 = \frac{(h_2 + h_3)v_m}{v_m + h_1\Delta z}, \quad k_2 = \frac{h_1 h_3 \Delta z}{v_m + h_1 \Delta z}, \quad k_3 = \frac{v_m}{v_m + h_1 \Delta z},$$

including the constant spatial step  $\Delta z = z_i - z_{i-1}$ . Eqn. (32) results in a system of DDEs of the form

$$d_t \mathbf{T}_m(t) = \mathbf{A}_m \mathbf{T}_m(t) + \mathbf{b}_{m,1} d_t T_{m,\text{in}}(t) + \mathbf{b}_{m,2} T_{m,\text{in}}(t) + \mathbf{D}_m \mathbf{T}_\infty(t),$$

with the corresponding system matrix  $\mathbf{A}_m \in \mathbb{R}^{n \times n}$ , input vectors  $\mathbf{b}_{m,1}$ ,  $\mathbf{b}_{m,2} \in \mathbb{R}^n$  and disturbance matrix  $\mathbf{D}_m \in \mathbb{R}^{n \times n}$ . The state  $\mathbf{T}_*$  can be noted with

$$\mathbf{T}_*(t) = (T_{*,1}^{\text{del}}(t), T_{*,2}^{\text{del}}(t), \dots, T_{*,n}^{\text{del}}(t))^T.$$

In order to eliminate the time derivative of the inflow temperature the transformation

$$\hat{\mathbf{T}}_m(t) = \mathbf{T}_m(t) - \mathbf{b}_{m,1} T_{m,\text{in}}(t)$$

is applied, which reveals the state space description

$$d_t \hat{\mathbf{T}}_m(t) = \mathbf{A}_m \hat{\mathbf{T}}_m(t) + (\mathbf{A}_m \mathbf{b}_{m,1} + \mathbf{b}_{m,2}) T_{m,\text{in}}(t) + \mathbf{D}_m \mathbf{T}_\infty(t).$$

In case of variable flow the previously described steps can be applied in a similar way. However, the system must be additionally discretized with respect to time, due to the time dependent slope of the characteristics.

## 5. Simulation and Experimental Validation

In this section the different modeling approaches are compared in simulation studies and validated with measurement data. All further analyses consider the medium to be water. The discussed models are the one-dimensional PDE-model (5) approximated by the FDM with a high resolution of 201 discretization points ( $n = 200$ ), the proposed DPDE-approach (29) with a low-order FDM approximation with 6 sampling points ( $n = 5$ ), named D(P)DE5, the DDE-model (10), the adapted DDE-model (11), and the D(P)DE1-model (31) derived from the proposed DPDE-model with 2 discretization points ( $n = 1$ ).

For a numerical comparison of the simulations and measurements the root-mean-square (RMS) error

$$E_2(z) = \sqrt{\frac{1}{p} \sum_{j=1}^p |T_*^j(z) - \tilde{T}_*^j(z)|^2}$$

and the maximum error metric

$$E_\infty(z) = \max_{1 < j < p} |T_*^j(z) - \tilde{T}_*^j(z)|$$

are introduced. Therein  $T_*$  and  $\tilde{T}_*$  denote the benchmark and simulation data at a specific spatial position  $z$  over all times  $j \in [t_1, t_p]$ , respectively.

The simulation study, identification, and validation is performed in Python.



Table 1: Used parameters for validation studies.

Parameter	Simulation	Measurement	Unit
$\rho_w$		7856	$\frac{\text{kg}}{\text{m}^3}$
$c_{p,w}$		500	$\frac{\text{J}}{\text{kg K}}$
$\lambda_w$		20	$\frac{\text{W}}{\text{m K}}$
$\rho_m$		997.04	$\frac{\text{kg}}{\text{m}^3}$
$c_{p,m}$		4179	$\frac{\text{J}}{\text{kg K}}$
$l$	5	1.62	m
$\epsilon$	0.7	0.91	-
$\alpha_{mw}$	1000	3052.87	$\frac{\text{W}}{\text{m}^2 \text{K}}$
$\alpha_{wa}$	80	46.98	$\frac{\text{W}}{\text{m}^2 \text{K}}$
$\alpha_{ma}$	73.39	46	$\frac{\text{W}}{\text{m}^2 \text{K}}$

### 5.1. Simulation study

The simulation study captures a scenario with a temperature ramp from 20 °C to 60 °C of the pipe input temperature  $T_{m,\text{in}}$  to unveil the main differences between the five approaches. Therefore, the high-order PDE-model is defined as benchmark. For the simulation a  $l = 5$  m long stainless steel pipe with an inner radius  $R_m = 7.7$  mm and an outer radius  $R_w = 10.65$  mm is considered. Moreover, a constant medium velocity of  $v_m = 0.5 \frac{\text{m}}{\text{s}}$  is assumed. Table 1 provides an overview of the physical parameters, which are chosen according to the common literature [22]. The heat transfer coefficient  $\alpha_{ma}$  of the DDE-model (11) is calculated by means of (7). Afterwards, the correction factor  $\epsilon$  is determined by means of a least squares optimization based on simulation results<sup>6</sup> of the benchmark model (cf. Table 1).

Figure 4 presents the results for a ramp input temperature  $T_{m,\text{in}}$ . It can be observed that the low order D(P)DE5-model reveals nearly the same results as the high-order PDE-model. Especially no numerical diffusion effects [23] due to the FDM approximation can be observed for the D(P)DE5-model. Moreover, a good coincidence can be also observed for the D(P)DE1. In contrast, the DDE-model and adapted DDE-model reveal a twenty respectively a ten times higher RMS error than the D(P)DE5-model. Compared with the D(P)DE1-model still an approximately four and two times higher RMS error (cf. Table 2) can be observed. Moreover, Table 2 reveals that the maximum error of the adapted DDE-model is 2.5 times higher than the maximum error of the D(P)DE1. Furthermore, the stationary inaccuracy of the DDE-model can be reduced using

<sup>6</sup>Note that a different scenario, where the input temperatures is decreased from 80 °C to 30 °C at a medium velocity of  $0.4 \frac{\text{m}}{\text{s}}$  is used for the identification.

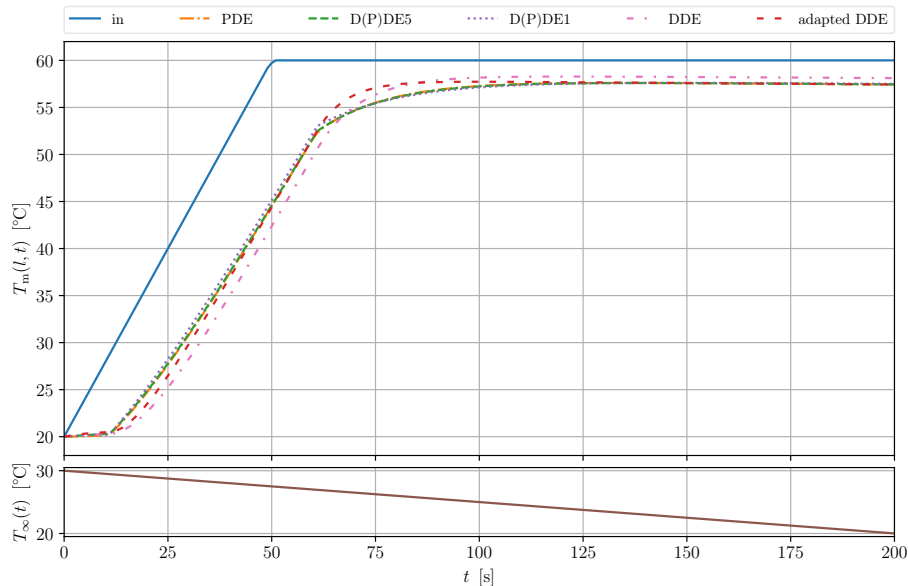


Figure 4: Medium temperature comparison of the new D(P)DE5-model, the PDE-model, and the DDE-approaches with a ramp for  $T_{m,in}$  at  $z = l$ .

Table 2: Error measures of D(P)DE5-, D(P)DE1-, adapted DDE- and DDE-model.

		DDE	adapted DDE	D(P)DE1	D(P)DE5	Units
medium	$E_2(l)$	1.2483	0.6435	0.3087	0.0619	°C
	$E_\infty(l)$	2.5454	1.6612	0.7077	0.1791	°C
wall	$E_2(l)$	-	-	0.2672	0.0849	°C
	$E_\infty(l)$	-	-	0.5907	0.1823	°C

the adapted DDE-model with adapted parameters.

Another advantage of the new DPDE-model is that the wall temperature can be reconstructed easily by means of (28). A comparison of the wall temperatures of the high-order PDE-model and the DPDE-models is presented in Figure 5.

## 5.2. Measurement

In this subsection the one-dimensional PDE-model (5), the new D(P)DE5-model (29), the adapted DDE-model, and the D(P)DE1-model (31) are experimentally validated. This was achieved by means of the test rig depicted in Figure 6, which was specifically designed for the validation of the analyzed modeling approaches. The pipe is filled with water. At each 0.54m both the medium temperature and the wall temperature are measured (cf. Figure 1). Thus, with a total length of 1.62m, four measuring points are available, the first of which is used as input temperature. Hence, three points are left for the validation. The medium and wall temperatures are measured by PT100 sensors

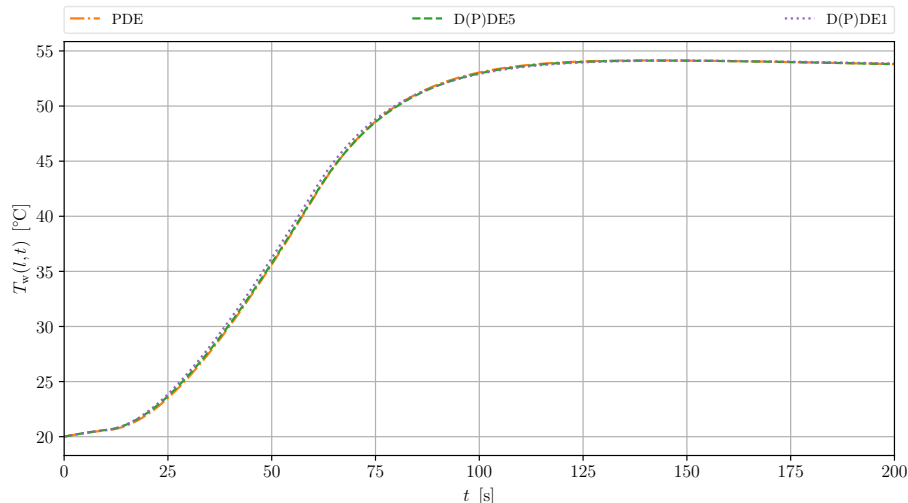


Figure 5: Wall temperature comparison of the new D(P)DE5-model, the PDE-model, and the DDE-approaches with a ramp for  $T_{m,in}$  at  $z = l$ .



Figure 6: Pipe test rig used for validation.

and thermocouples, respectively. Furthermore, the volume flow rate through the pipe is measured by applying the principle of differential pressure and the ambient temperature is measured by another thermocouple. The signal processing is done by an Arduino Uno complemented with appropriate sensor boards. Due to its slow variation the ambient temperature is set to a constant value of 25.8 °C. Moreover, the dynamics of the PT100 sensors are compensated by means of an inverse model. The pipe under consideration has an inner diameter of 3/5 inch and an outer diameter of 4/5 inch. Figure 8 - 10 and Table 3 present the validation results, where the input temperature and the volume flow rate are varied. The required heat transfer coefficients  $\alpha_{mw}$ ,  $\alpha_{wa}$ , and the correction parameter  $\epsilon$  are determined by a least squares optimization based on the measured medium and wall temperatures at the pipe outlet. Afterwards, the heat transfer coefficient  $\alpha_{ma}$  is computed by evaluating (7) with the identified values of  $\alpha_{mw}$  and  $\alpha_{wa}$ . For this purpose, another data set is used (cf. highlighted sector in Figure 7), where the velocity of the medium is nearly constant. The identified and computed parameters are given in Table 1. Figure 8 presents the measured input and output temperature, the medium velocity, and the simulated output temperatures. An almost perfect match of all models with the measured output can be observed. Based on the error measures presented in Table 3 one can observe that the D(P)DE5-model reveals the smallest average error. However, if just the medium temperature at the output of the pipe is required each of the

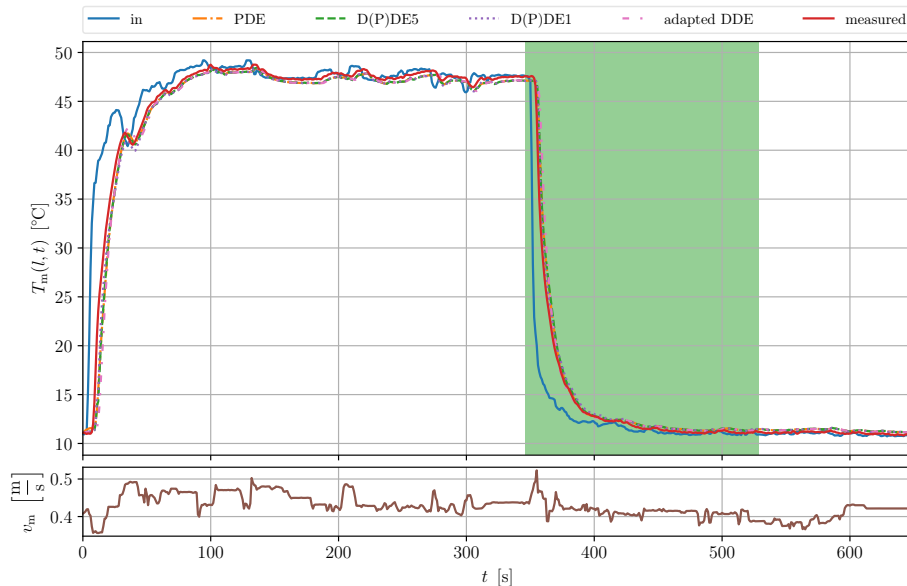


Figure 7: Measurement with green marked data, that is used for the identification of the parameters  $\alpha_{mw}$ ,  $\alpha_{wa}$ ,  $\alpha_{ma}$  and  $\epsilon$ .

models is applicable. In contrast, if the wall temperature or an intermediate medium temperature is needed the D(P)DE5-model or its simplest solution, the D(P)DE1, are a good alternatives to the PDE-model.<sup>7</sup> Furthermore, at  $z = l/3$  all the newly proposed models show a perfect match with the measured data (cf. Figure 10), whereas the error of the adapted DDE-model increases. A spatially dependent definition (resp. identification) of the correction factor  $\epsilon$  may lead to better results. Moreover, the wall temperatures calculated by the PDE- and the D(P)DE5-model show a similar behavior as the measurement. The occurring offset of 2 °C (compare Figure 9 between 100s to 180s) is likely to be caused by the nonlinear behavior of the thermocouple, which is not compensated. At different measuring points different offsets (positive and negative) arise.

To sum up, the proposed modeling approaches succeed in reproducing the measurements in the considered scenario. Furthermore, in contrast to the classical DDE-approach, the PDE-model and the DPDE-approaches admit for the additional computation of the wall temperature.

<sup>7</sup>Using (31) or (11) for a temperature calculation at a point  $z_0 < l$  of the pipe, the length  $l$  has to be replaced by the chosen point  $z_0$ . Thus, the shell surface area in (11) is changing too.

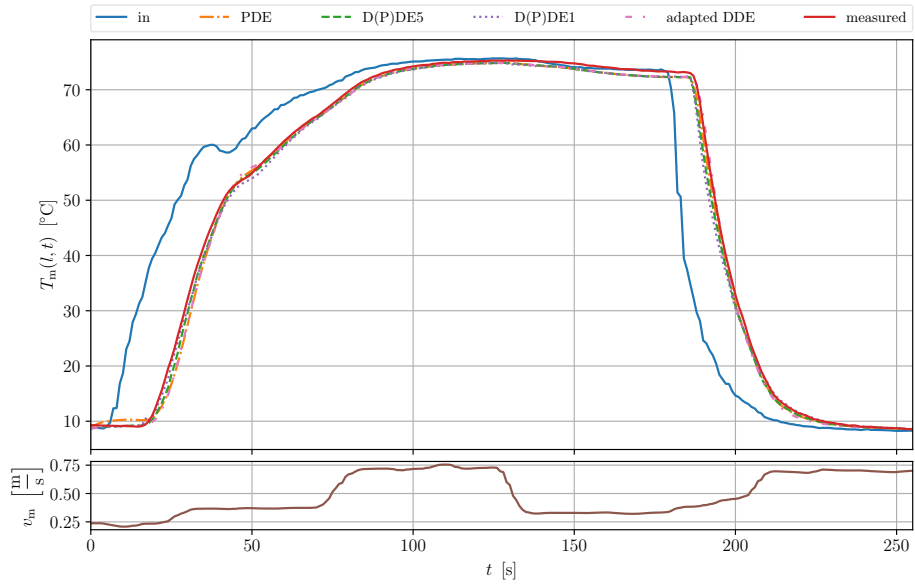


Figure 8: Medium temperature comparison of the new D(P)DE5-model, the PDE-model, and the DDE-approaches with measurement data at  $z = l$ .

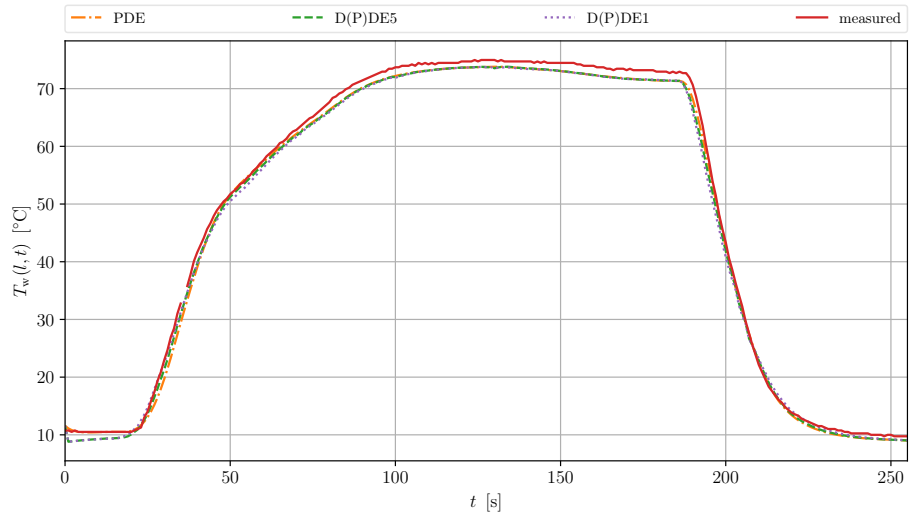


Figure 9: Wall temperature comparison of the new D(P)DE5-model and the PDE-model with measurement data at  $z = l$ .

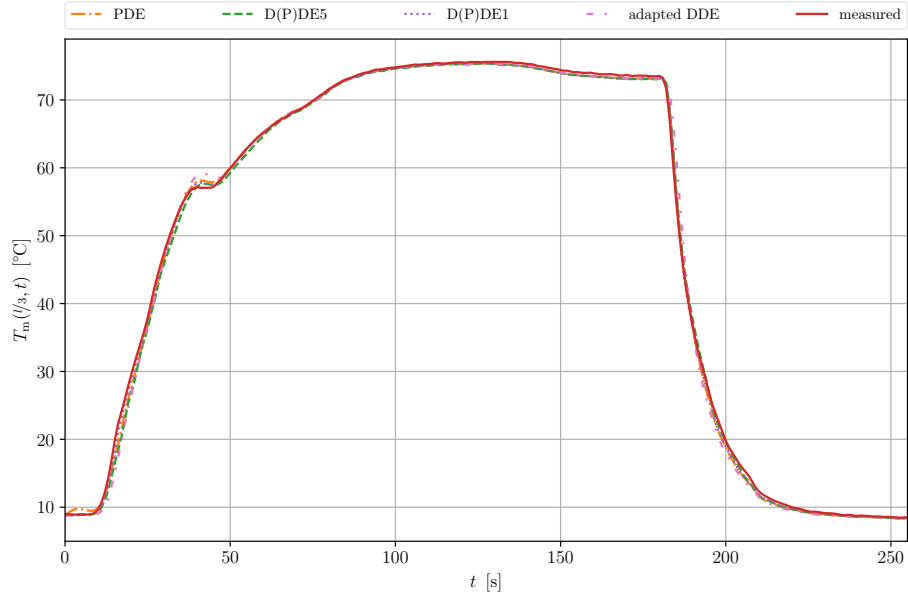


Figure 10: Medium temperature comparison of the new D(P)DE5-model, the PDE-model, and the DDE-models with measurement data at  $z = l/3$ .

Table 3: Numerical comparison of adapted DDE-, D(P)DE5-, D(P)DE1- and PDE-model against measurement data.

		adapted DDE	D(P)DE1	D(P)DE5	PDE	Unit
medium	$E_2(l)$	1.2605	1.4289	1.1913	1.2876	$^{\circ}\text{C}$
	$E_{\infty}(l)$	4.7591	7.3504	5.0512	5.0342	$^{\circ}\text{C}$
	$E_2(l/3)$	1.2869	0.4921	0.8212	0.6690	$^{\circ}\text{C}$
	$E_{\infty}(l/3)$	6.8591	2.0078	3.9308	2.9872	$^{\circ}\text{C}$
wall	$E_2(l)$	-	2.5682	2.4378	2.3330	$^{\circ}\text{C}$
	$E_{\infty}(l)$	-	33.0015	32.7530	31.3974	$^{\circ}\text{C}$

## 6. Conclusion and Further Work

### 6.1. Conclusion

This contribution presents a physical derivation of commonly used DDE-models describing the thermal behavior of a plug flow through a pipe, where a heat transfer between the transport medium and the wall and between the wall and the ambient is considered explicitly. Starting from a one-dimensional PDE-model for the fluid inside the pipe and a two-dimensional PDE-model for the wall of the pipe a one-dimensional PDE-model is derived. Based on the latter one a novel DPDE-model is introduced, which is a combination of the PDE- and DDE-approach. On the basis of the DPDE-model a new version of the well known DDE-model is derived. It is shown that the common heuristic approach has to be extended by a tuning parameter to be able to cover the pipe dynamics. In contrast no tuning parameter has to be applied to the proposed DPDE-model and the new DDE-approach. Moreover, the new DPDE-model allows to calculate the wall temperature at any position. The different models are compared in simulation to illustrate their strengths and weaknesses. It has been shown that for highly transient changes at the input the new modeling approach delivers better results than the common DDE-approach. Compared with a FDM simulation of the one-dimensional PDE no numerical diffusion effect can be observed for the new approach. Finally, a validation against measurements shows an almost perfect match of all modeling approaches.

### 6.2. Further work

In a first step the introduced DPDE-model can be used to observe the temperature profile in plug flow tube reactors (e.g. in a catalyst). The obtained DPDE-model forms the basis for an input-output description for temperature of the medium involving measured boundary quantities only. The model forms an appropriate basis for the identification of the heat transfer coefficients, if the latter are unknown. In contrast to alternative schemes, which require numerically expensive optimization an comparably simple approach [24] can be used, which requires only very basic optimization algorithms. Furthermore, the observed data can be used to govern such profiles by appropriate control algorithms. In addition the applicability of the DPDE-model to pipe networks will be investigated in the future. Finally, in view of applications with non-turbulent flow regimes the a priori spatially one-dimensional modeling approaches are likely to be not sufficiently accurate. This motivates further investigations on the basis of higher dimensional stationary-flow regimes as studied numerically for example in [25].

## 7. Acknowledgments

The present contribution is a result of the research project MoReNe (FFG-Nr. 864725) funded by the Austrian Research Promotion Agency (FFG) and Innio Jenbacher GmBH & Co OG located in Jenbach (Austria). The authors gratefully acknowledge Jonathan Halmen, who has set up the long pipe test rig and recorded the measurements.

## Appendix A. Approximate heat transfer coefficients

Within this section the calculation of the overall heat transfer coefficients for the defined mean temperature (4) is explained. The stationary solution of (2) satisfies

$$\partial_r (r\dot{q}(r, z)) = 0, \quad \dot{q}(r, z) = -\lambda_w \partial_r T_w(r, z).$$

Integrating the first of these equations w.r.t.  $r$  over the interval  $[R_m, r]$  leads to

$$r\dot{q}(r, z) - R_m\dot{q}(R_m, z) = 0.$$

With  $\dot{q}(r, z) = -\lambda_w \partial_r T_w(r, z)$  one obtains

$$\lambda_w r \partial_r T_w(r, z) + R_m \dot{q}(R_m, z) = 0.$$

Solving this ODE for  $r \mapsto T_w(r, z)$  yields

$$\lambda_w (T_w(r, z) - T_w(R_m, z)) = \ln \left( \frac{R_m}{r} \right) R_m \dot{q}(R_m, z).$$

The latter equation is integrated over  $A_w$

$$\int_{R_m}^{R_w} 2\pi r \lambda_w (T_w(r, z) - T_w(R_m, z)) \, dr = 2\pi R_m \dot{q}(R_m, z) \int_{R_m}^{R_w} r \ln \left( \frac{R_m}{r} \right) \, dr$$

to obtain

$$\begin{aligned} A_w \lambda_w (\bar{T}_w(z) - T_w(R_m, z)) \\ = 2\pi R_m \left( R_w^2 \ln \left( \frac{R_w}{R_m} \right) + \frac{1}{2} (R_m^2 - R_w^2) \right) \dot{q}(R_m, z). \end{aligned}$$

The latter equation can be simplified by substituting  $A_w = \pi(R_w^2 - R_m^2)$  and eliminating  $T_w(R_m, z)$  by means of the boundary condition (3b). This finally yields

$$T_m(z) - \bar{T}_w(z) = \left( \frac{1}{\alpha_{mw}} + \frac{\bar{R}_m}{\lambda_w} \right) \dot{q}(R_m, z) \quad (\text{A.1})$$

with

$$\bar{R}_m = R_m \left( \frac{R_w^2}{R_w^2 - R_m^2} \ln \left( \frac{R_w}{R_m} \right) - \frac{1}{2} \right).$$

Similar computations for the outer boundary of the jacket lead to

$$\bar{T}_w(z) - T_\infty = \left( \frac{1}{\alpha_{wa}} + \frac{\bar{R}_w}{\lambda_w} \right) \dot{q}(R_m, z), \quad (\text{A.2})$$



with

$$\bar{R}_w = R_m \left( -\frac{R_m^2}{R_w^2 - R_m^2} \ln \left( \frac{R_w}{R_m} \right) + \frac{1}{2} \right).$$

Summing up (A.1) and (A.2) reveals

$$T_m(z) - T_\infty = \dot{q}(R_m, z) \left( \frac{1}{\alpha_{mw}} + \frac{1}{\alpha_{wa}} + \frac{R_m}{\lambda_w} \ln \left( \frac{R_w}{R_m} \right) \right)$$

the well known formulation of the overall heat transfer for a cylindrical pipe (cf. [17, p. 31 ff.]).

## References

- [1] T. L. Santos, L. Roca, J. L. Guzman, J. E. Normey-Rico, M. Berenguel, Practical mpc with robust dead-time compensation applied to a solar desalination plant, *IFAC Proceedings Volumes* 44 (1) (2011) 4909–4914.
- [2] P. Jie, Z. Tian, S. Yuan, N. Zhu, Modeling the dynamic characteristics of a district heating network, *Energy* 39 (1) (2012) 126–134.
- [3] T. Qiu, X. Li, H. Liang, X. Liu, Y. Lei, A method for estimating the temperature downstream of the scr (selective catalytic reduction) catalyst in diesel engines, *Energy* 68 (2014) 31–317. doi:10.1016/j.energy.2014.02.101.
- [4] O. Lepreux, Model-based Temperature Control of a Diesel Oxidation Catalyst, Ph.D. thesis, École Nationale Supérieure des Mines de Paris (2009).
- [5] O. Lepreux, Y. Creff, N. Petit, Model-based control design of a diesel oxidation catalyst, *IFAC Proceedings Volumes* 42 (11) (2009) 279–284.
- [6] S. Bachler, J. Huber, H. Kopecek, F. Woittennek, Control of Cooling Loops with Large and Variable Delays, 1<sup>st</sup> IEEE Conference on Control Technology and Applications.
- [7] C. M. Cirre, M. Berenguel, L. Valenzuela, E. F. Camacho, Feedback linearization control for a distributed solar collector field, *Control Engineering Practice* 15 (12) (2007) 1533–1544. doi:10.1016/j.conengprac.2007.03.002.  
URL <http://www.sciencedirect.com/science/article/pii/S096706610700055X>
- [8] R. Kicsiny, New delay differential equation models for heating systems with pipes, *International Journal of Heat and Mass Transfer* 79 (2014) 807–815. doi:10.1016/j.ijheatmasstransfer.2014.08.058.
- [9] O. Lepreux, Y. Creff, N. Petit, Model-based temperature control of a diesel oxidation catalyst, *Journal of Process Control* 22 (1) (2012) 41–50.

- [10] R. Kicsiny, Grey-box model for pipe temperature based on linear regression, *International Journal of Heat and Mass Transfer* 107 (2017) 13–20.
- [11] L. Pekař, R. Prokop, Algebraic robust control of a closed circuit heating-cooling system with a heat exchanger and internal loop delays, *Applied Thermal Engineering* 113 (2017) 1464–1474.
- [12] N. Bekiaris-Liberis, M. Krstic, *Nonlinear Control Under Nonconstant Delays*, SIAM, 2013.
- [13] H. Mounier, J. Rudolph, Flatness-based control of nonlinear delay systems: A chemical reactor example, *International Journal of Control* 71 (5) (1998) 871–890. [arXiv:http://dx.doi.org/10.1080/002071798221614](http://dx.doi.org/10.1080/002071798221614), [doi:10.1080/002071798221614](https://doi.org/10.1080/002071798221614).  
URL <http://dx.doi.org/10.1080/002071798221614>
- [14] T. Witelski, M. Bowen, *Methods of Mathematical Modelling: Continuous Systems and Differential Equations*, Springer International Publishing, 2015. [doi:10.1007/978-3-319-23042-9](https://doi.org/10.1007/978-3-319-23042-9).
- [15] T. L. Bergman, F. P. Incropera, *Fundamentals of Heat and Mass Transfer*, Wiley, 2011.  
URL <http://books.google.de/books?id=vvyIoXEywMoC>
- [16] H. Aschemann, R. Prabel, C. Gross, D. Schindele, Flatness-based control for an internal combustion engine cooling system, in: (ICM), 2011 IEEE International Conference on Mechatronics, 2011, pp. 140–145. [doi:10.1109/ICMECH.2011.5971271](https://doi.org/10.1109/ICMECH.2011.5971271).  
URL <http://ieeexplore.ieee.org/stamp/stamp.jsp?arnumber=5971271>
- [17] H. D. Baehr, K. Stephan, *Heat and Mass Transfer*, Springer Science + Business Media, 2011. [doi:10.1007/978-3-642-20021-2](https://doi.org/10.1007/978-3-642-20021-2).
- [18] S. Bachler, J. Huber, F. Woittennek, Zur thermischen Modellierung inkompressibler Rohrströmungen, *at - Automatisierungstechnik* 65 (8).
- [19] D. Bresch-Pietri, N. Petit, Implicit integral equations for modeling systems with a transport delay, in: E. Witrant, E. Fridman, O. Sename, L. Dugard (Eds.), *Recent results on time-delay systems: Analysis and control*, Vol. 5 of *Analysis and Control*, 2016.  
URL <https://hal.archives-ouvertes.fr/hal-01384486>
- [20] R. Courant, D. Hilbert, *Methods of Mathematical Physics II, Methods of Mathematical Physics*, Interscience Publishers, 1962.
- [21] F. John, *Partial Differential Equations*, Applied Mathematical Sciences, Springer New York, 1991.  
URL [https://books.google.at/books?id=cBib\\_bsGGLYC](https://books.google.at/books?id=cBib_bsGGLYC)

- [22] W. Rohsenow, J. Hartnett, Y. Cho, Handbook of heat transfer, McGraw-Hill handbooks, McGraw-Hill, 1998.
- [23] B. Andersson, R. Andersson, L. Håkansson, M. Mortensen, R. Sudiyo, B. van Wachem, Computational Fluid Dynamics for Engineers, Cambridge University Press, 2011.
- [24] T. Knüppel, F. Woittennek, A contribution to parameter identification in infinite-dimensional systems, 2013 European Control Conference (ECC) (2013) 1591–1596.
- [25] Y. Cao, X. Gao, R. Li, A liquid plug moving in an annular pipe - heat transfer analysis, International Journal of Heat and Mass Transfer 139 (2019) 1065–1076.